Developmental Cell
Article

A bHLH Complex Controls Embryonic Vascular Tissue Establishment and Indeterminate Growth in *Arabidopsis*

Bert De Rybel,[1,4] Barbara Möller,[1,4] Saiko Yoshida,[1] Ilona Grabowicz,[1] Pierre Barbier de Reuille,[3] Sjef Boeren,[1] Richard S. Smith,[3] Jan Willem Borst,[1,2] and Dolf Weijers[1,*]
[1]Laboratory of Biochemistry
[2]Microspectroscopy Center
Wageningen University, Dreijenlaan 3, 6703HA Wageningen, The Netherlands
[3]Institute of Plant Sciences, University of Bern, Altenbergrain 21, Bern CH-3013, Switzerland
[4]These authors contributed equally to this work
*Correspondence: dolf.weijers@wur.nl
http://dx.doi.org/10.1016/j.devcel.2012.12.013

SUMMARY

Plants have a remarkable potential for sustained (indeterminate) postembryonic growth. Following their specification in the early embryo, tissue-specific precursor cells first establish tissues and later maintain them postembryonically. The mechanisms underlying these processes are largely unknown. Here we define local control of oriented, periclinal cell division as the mechanism underlying both the establishment and maintenance of vascular tissue. We identify an auxin-regulated basic helix-loop-helix (bHLH) transcription factor dimer as a critical regulator of vascular development. Due to a loss of periclinal divisions, vascular tissue gradually disappears in bHLH-deficient mutants; conversely, ectopic expression is sufficient for triggering periclinal divisions. We show that this dimer operates independently of tissue identity but is restricted to a small vascular domain by integrating overlapping transcription patterns of the interacting bHLH proteins. Our work reveals a common mechanism for tissue establishment and indeterminate vascular development and provides a conceptual framework for developmental control of local cell divisions.

INTRODUCTION

Plants maintain the ability to grow indeterminately after embryogenesis, through continuous division of initial cells, which are often referred to as stem cells (Weigel and Jürgens, 2002). This indeterminate growth, which we refer to as indeterminacy, is required to maintain tissues in a growing organism, and loss of the underlying divisions causes the tissue to differentiate (determinacy). Lineage tracing suggests that initials for each of the three major tissues (epidermis, ground tissue, and vascular tissue) are specified early during embryogenesis (Scheres et al., 1994). Because plant cells do not migrate, strict control of division in tissue-specific initials should be essential for tissue formation and for the continued indeterminate postembryonic growth of that tissue. Indeed, the first examples of cell division control by root developmental regulators were recently observed during ground tissue (Sozzani et al., 2010) and epidermis/lateral root cap (Dhonukshe et al., 2012) maintenance. Nevertheless, a key unanswered question is, how do these tissues initially form in the embryo? Furthermore, because most developmental regulators accumulate in larger domains (Dhonukshe et al., 2012; Sozzani et al., 2010), it is unclear how their activity is spatially restricted to control cell division behavior.

Very few potential regulators of tissue formation in the embryo have been identified to date. Among these, however, the transcription factor MONOPTEROS/AUXIN RESPONSE FACTOR5 (MP/ARF5; Hardtke and Berleth, 1998) offers a good starting point to dissect the process of tissue formation in the embryo. *mp* mutants do not make an embryonic root (Hardtke and Berleth, 1998), and although tissue formation in this mutant has not been described in detail, several of its recently identified targets are exclusively expressed in the vascular tissue (Donner et al., 2009; Schlereth et al., 2010). Hence, because MP has been shown to regulate vascular tissue development in leaves (Donner et al., 2009; Scarpella and Helariutta, 2010) and stems (Przemeck et al., 1996), it likely contributes to the formation of vascular tissue in the embryo.

Vascular tissues are comprised of two conducting cell types (phloem and xylem) and intervening cambium cells that can generate conducting cell types (reviewed in Scarpella and Helariutta, 2010). Depending on the organ, these three cell types are arranged in particular ways, yet these arrangements are both ancient and evolutionary conserved among vascular plants (Kenrick and Crane, 1997). In *Arabidopsis*, all vascular tissues of the plant axis (root and hypocotyl) are derived from only four initial cells in the globular embryo (Scheres et al., 1994). Upon their specification, these cells must undergo longitudinal (also termed periclinal, because the cells are parallel to the main axis) divisions to increase the number of cell files and layers in the mature embryo. In addition, periclinal divisions occur postembryonically in the procambium and phloem of the postembryonic root meristem to increase the number of vascular cell files (Mähönen et al., 2000). Although a few genes have been shown

to be required for promoting (WOODEN-LEG [WOL; Mähönen et al., 2000] and LONESOME HIGHWAY [LHW; Ohashi-Ito and Bergmann, 2007]) or inhibiting (HD-ZIP III; Carlsbecker et al., 2010) the number of cell files in vascular tissue in the growing postembryonic root, at present it is unclear how the establishment of this tissue during embryogenesis is controlled. Consequently, it is not known whether embryonic tissue formation and postembryonic growth share a common mechanism. Finally, because the mutations that have been reported to affect the number of vascular cell files do not necessarily affect the ability to grow indeterminately, the significance of periclinal divisions in this tissue remains to be determined.

Here we identify a module involving MP, the direct MP target TARGET OF MONOPTEROS5 (TMO5), and its basic helix-loop-helix (bHLH) interactor, LHW, that is both necessary and sufficient for the periclinal cell divisions that underlie the establishment and indeterminacy of the vascular tissue. Our work identifies key regulators of vascular tissue establishment in the plant embryo and reveals a mechanism for the control of indeterminate tissue growth through local, oriented cell division.

RESULTS

TMO5 Controls Vascular Tissue Initiation

Although MP activity has been shown to be critical for vascular tissue development in postembryonic stages (Donner et al., 2009; Przemeck et al., 1996), its role in the earliest steps of tissue establishment has not been studied. In previous work, several vascular tissue-specific genes (e.g., *TMO5* and *ATHB8*) were identified as direct targets of MP (Donner et al., 2009; Schlereth et al., 2010). These genes are activated in vascular tissues at its first establishment, and expression is strongly downregulated in *mp* mutant embryos, raising the possibility that MP controls vascular initiation.

Because the arrangement of the small vascular cells in early embryos is difficult to interpret by conventional microscopy, we devised a three-dimensional (3D) imaging and cellular segmentation procedure. In wild-type (WT), the four vascular initial cells of the globular-stage embryo all divide periclinally (along the main body axis) to give rise to two concentric cell layers (91%, n = 33; Figures 1A and 1B). Subsequently, the outer cells all divide periclinally to increase their numbers within the layer (100%, n = 30; Figures 1C and 1D). Later, cells in both the outer and inner cell layers divide periclinally, but less regularly, to increase cell file numbers (Figure 1E). In contrast, *mp* mutant embryos contained much fewer cell files in the vascular tissue, and the number of cells within these files was not dramatically altered (Figure 1F). Hence, MP is required for periclinal cells divisions during early vascular tissue establishment.

The MP target gene *TMO5* encodes a bHLH transcription factor that is first expressed in all four vascular initials (Figures 1G and 1H; Figure S1K available online) and later becomes restricted to the xylem precursor cells in both the embryo (Figure 1I) and root (Figures S1F and S1G), and thus represents a good candidate for mediating MP function in vascular initiation. We compared early embryos of *mp*-S319 and *mp*-S319 in which TMO5 activity was restored with a pMP-TMO5 transgene (Schlereth et al., 2010), and found that this transgene significantly suppressed the vascular initiation defect of the *mp* mutant (chi-square p value = 0.003; Table S1). Therefore, TMO5 mediates MP-dependent vascular tissue initiation.

Because the bHLH transcription factor TMO7 shows the same initial gene expression pattern but the protein is transported to the adjacent hypophysis (Schlereth et al., 2010), we first investigated TMO5 protein localization. The accumulation of pTMO5-TMO5-3-green fluorescent protein (pTMO5-TMO5-3GFP), pTMO5-TMO5-tandemTomato (tdTomato), and pTMO5-TMO5-yellow fluorescent protein (pTMO5-TMO5-YFP) translational fusion proteins exactly matched previously described *TMO5* messenger RNA (mRNA) and p*TMO5-n3GFP* (nuclear triple GFP) reporter patterns (Schlereth et al., 2010) in globular-stage embryos (Figures S1D and S1E) and mature roots (Figures S1H–S1J). Because pTMO5-TMO5-3GFP protein is active in complementing mutant phenotypes (see below), this suggests that TMO5 function does not depend on protein mobility. Indeed, although MP is also expressed in other tissues (Schlereth et al., 2010), local inhibition of MP activity through expression of the inhibitor bdl only in vascular and ground tissue precursors is sufficient to induce the same vascular defect (Figures S1A and S1B). Hence, the auxin-MP-TMO5 module acts in vascular initiation during embryogenesis.

To determine the role of TMO5 in vascular tissue initiation, we analyzed insertion mutants (Figures S2E and S2F). Because *tmo5* single mutants did not display any phenotypes (Schlereth et al., 2010), we created a double mutant with its closest homolog, *TMO5-LIKE1* (*T5L1*; At1g68810). The T5L1 protein is 48% identical to TMO5 (Figures S2A–S2D), and the gene shows MP-dependent expression in transcript profiling (Schlereth et al., 2010) and is expressed in the vasculature of the embryo (Figure 1J). In *tmo5 t5l1* double-mutant embryos, we found a striking defect in the periclinal vascular divisions (45%, n = 11; Figures 1K–1N), leading to a vascular tissue with fewer cells dividing at abnormal planes (Figures 1M and 1N). Consistent with this role in increasing cell file numbers, the vascular tissue of mature embryos (Figures 1O and 1P) and postembryonic roots (Figures 1Q and 1R) was reduced in diameter in the double mutant and contained fewer cells. Vascular tissue encompasses two conducting cell types: phloem and xylem (Scarpella and Helariutta, 2010). In WT roots, a bisymmetric pattern of two phloem poles and two protoxylem poles can be observed (100%, n = 32; Figure 1Q; Table S2). The reduced vascular tissue in double-mutant roots contained only one phloem pole and one protoxylem pole (93%, n = 87; Figure 1R; Table S2). The phenotypes were fully complemented by the introduction of pTMO5-TMO5-3GFP fusion protein (100%, n = 51; Table S2). We conclude that TMO5 and T5L1 act downstream of MP to control the divisions of the first vascular initials and their daughter cells (Figure 1S), and hence the establishment of the vascular tissue.

TMO5 Forms a bHLH Dimer with LHW In Vivo

The phenotype of the postembryonic *tmo5 t5l1* mutant is very similar to that of the previously described *lhw* mutant (Ohashi-Ito and Bergmann, 2007). Indeed, in our hands, the root phenotypes of *lhw* and *tmo5 t5l1* were indistinguishable (Figure S3; Table S2). *LHW* encodes a bHLH transcription factor that is phylogenetically distant from TMO5 (<10% identity; Figures S2A–S2D), and yeast-two-hybrid data suggest a

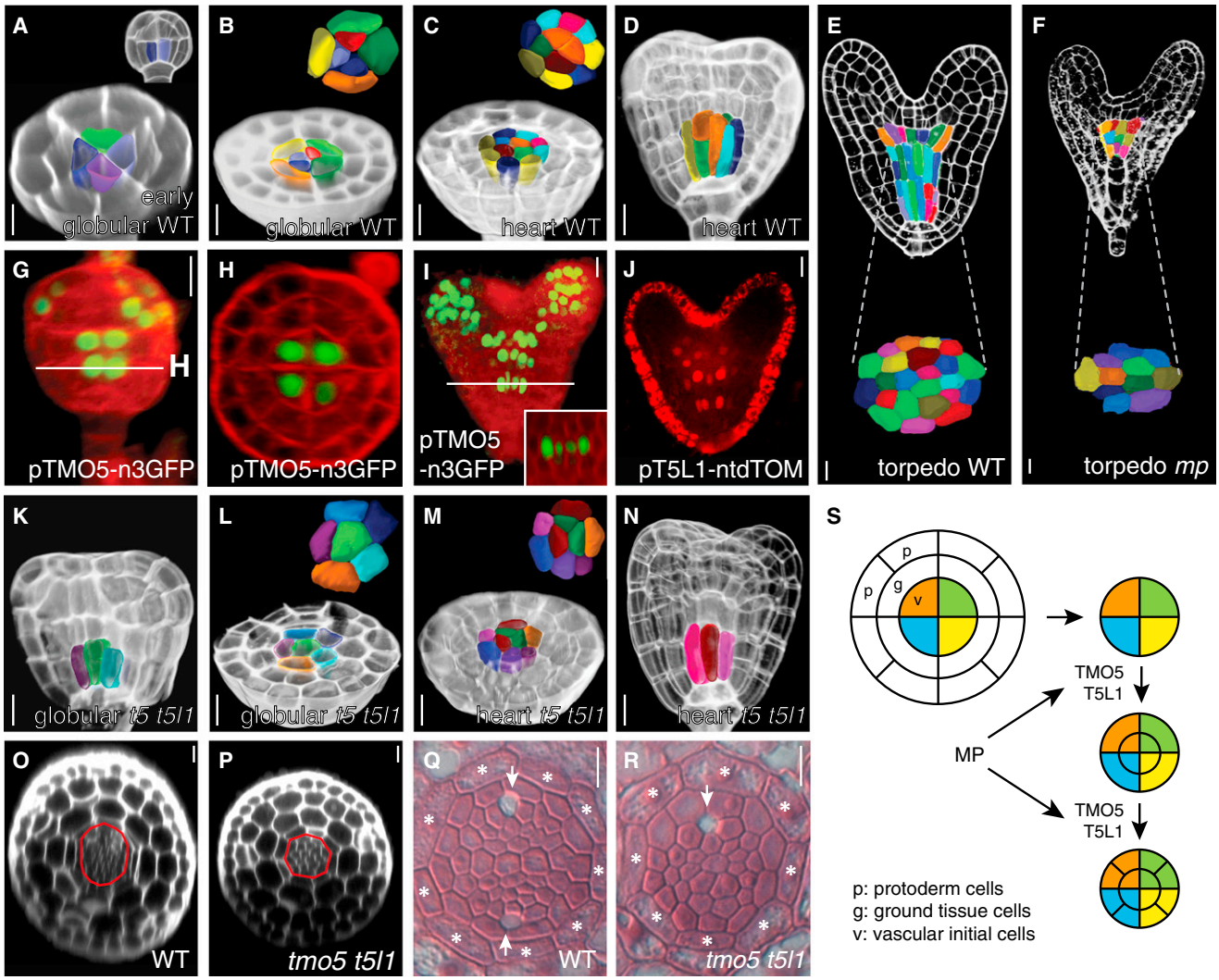

Figure 1. Vascular Phenotypes of *mp* and *tmo5 tmo5-like1* Double Mutants

(A–F) 3D reconstructions of WT (n = 5, 100%) (A–E) and *mp* mutant (n = 5, 100%) (F) embryos with vascular cell volumes highlighted.

(G–J) Expression of pTMO5-n3GFP (G–I; inset in I is cross-section) and pT5L1-ntdTomato (J) in globular-stage (G and H) and heart-stage (I and J) embryos.

(K–N) 3D reconstructions of *t5 t5l1* mutant (n = 11, 45%) embryos. Insets in (B), (C), (E), (F), (I), (L), and (M) show cross-sections.

(O and P) Optical cross-sections through the root of mature WT (O) and *tmo5 t5l1* double-mutant (P) embryos.

(Q and R) Cross-sections of postembryonic roots of WT (Q) and *tmo5 t5l1* double mutant (R). Asterisks indicate endodermis, and arrows indicate phloem pole.

(S) Schematic representation of the lineage in WT, indicating which steps are controlled by MP, TMO5, and T5L1.

Scale bar represents 10 μm in all panels. See also Figure S1 and Table S1.

potential interaction between LHW and TMO5 (Ohashi-Ito and Bergmann, 2007). Because it has been shown that bHLH proteins often need to dimerize in order to bind DNA (Massari and Murre, 2000), we used an unbiased immunoprecipitation (IP)-mass spectrometry (MS) strategy to identify in vivo pTMO5-TMO5-3GFP protein complexes in siliques. After quantification and statistical analysis (see Experimental Procedures), we found TMO5 and GFP to be the most abundant proteins in the immunocomplex, confirming the quality of the analysis (Table S3). Strikingly, LHW was identified in the TMO5 complex as the next most-abundant protein, and in addition, LHW-LIKE2 (LL2; At2g31280) was also recovered (Figure 2A; Table S3). We next performed the reciprocal IP-MS experiment on pLHW-LHW-YFP siliques and seedling roots, and recovered TMO5, T5L1, and TMO5-LIKE3 (T5L3) as interactors (Figure 2A; Table S3). To determine whether the observed interactions were direct protein-protein interactions, we used a fluorescence resonance energy transfer (FRET)-fluorescence lifetime imaging (FLIM) interaction analysis of cyan fluorescent protein (CFP)- and YFP-tagged proteins expressed in a transient *Arabidopsis* leaf mesophyll protoplast system (Figures 2B–2D). We detected interactions between all TMO5 and LHW subclade members analyzed (Figure 2E). These data confirm that heterodimers between TMO5 and LHW bHLH clades exist in planta, and genetic data suggest that both partners act to positively control the same process.

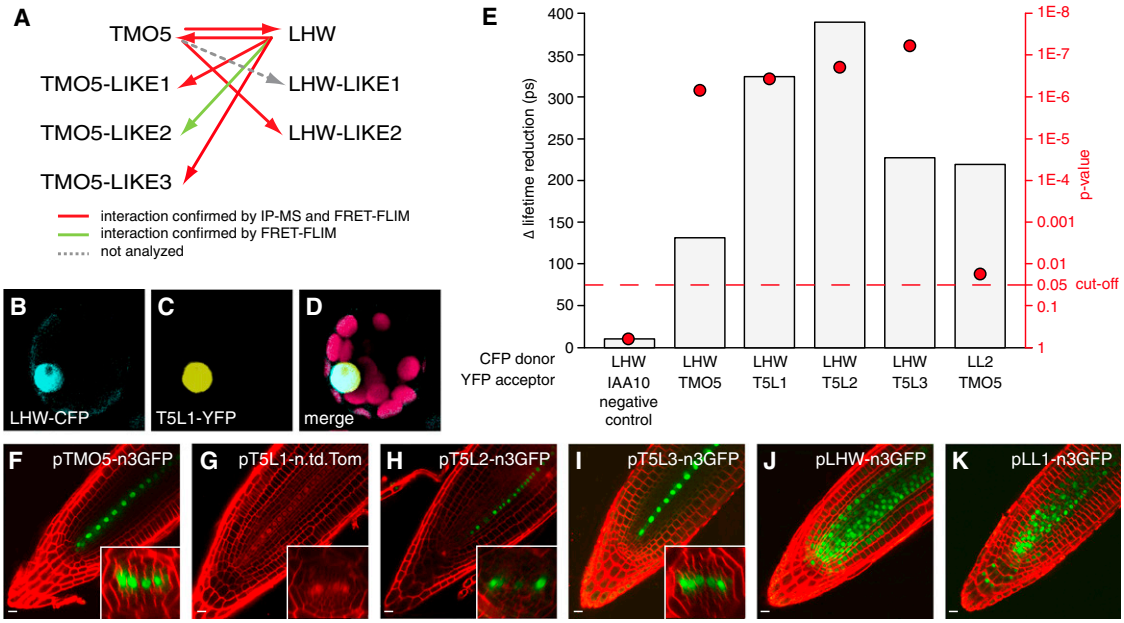

Figure 2. Members of the TMO5 and LHW Subclades Interact In Vivo

(A) Interactions between TMO5 and LHW subclade members as determined by IP-MS and/or FRET-FLIM.

(B–D) Expression of T5L1-YFP (B) and LHW-CFP (C) and merge with chloroplasts (D) in protoplasts.

(E) CFP lifetime reduction (gray bars, picoseconds, left y axis) and p values (red dots, right y axis) for FRET interactions. IAA10-YFP was used as negative control.

(F–K) Expression of p*TMO5-n3GFP* (F), p*T5L1-ntdTomato* (G), p*T5L2-n3GFP* (H), p*T5L3-n3GFP* (I), p*LHW-n3GFP* (J), and p*LL1-n3GFP* (K) in the root meristem. Insets in (F)–(I) show cross-sections through the root meristem.

Scale bar represents 10 μm. See also Figure S2 and Table S3.

TMO5/LHW Dimers Control the Indeterminate Growth of Vascular Tissue

To determine which of the TMO5 and LHW clade proteins could contribute to vascular development, we analyzed the expression pattern of all of the genes. Importantly, all *TMO5* subclade members showed expression in the xylem precursor cells of the root meristem (Figures 2G–2I, S1K, and S1L) similarly to *TMO5* (Figures 2F and S1M). In striking contrast to these highly specific expression patterns, *LHW* and *LHW-LIKE1* (*LL1*) were more broadly expressed in embryos (Figures 3I, 3J, and S1N) and in root meristems (Figures 2J and 2K), whereas no *LL2* expression could be observed in the embryo and root.

Given the coexpression and in vivo interaction between TMO5 and LHW subclades, we determined the consequences of further reducing the function of either of the two subclades by creating higher-order mutants with strongly reduced transcript levels (Figures S2E and S2F). None of the double- or triple-mutant combinations that we generated in the *TMO5* subclade showed defects unless both *tmo5* and *tmo5-like1* mutations were present (Table S2). This suggests that *TMO5* and *T5L1* are the main regulators of vascular development, whereas *TMO5-LIKE2* (*T5L2*) and *T5L3* do not make major contributions in an otherwise WT background. Interestingly, however, *tmo5 t5l1 t5l3* triple mutants and *tmo5 t5l1 t5l2 t5l3* quadruple mutants displayed dramatic vascular phenotypes that increased in severity upon removal of more clade members (Figures 3A–3E and S3; and Table S2). In *tmo5 t5l1 t5l3* triple mutants, the vascular tissue in the root meristem was reduced in size relative to the *tmo5 t5l1* double mutant (Figures 3D and S3). In quadruple *tmo5 t5l1 t5l2 t5l3* mutants, we did not observe any differentiated vascular tissue along the root (Figure S3). The reduction in root length correlated with the number of genes that were mutated (Figure 3A). Strikingly, *lhw ll1* double mutants showed defects that were intermediate between the triple and quadruple mutants in the *TMO5* subclade (Figures 3A, 3F, 3G, and S3). In all mutants, the epidermis and endodermis differentiated normally, as judged by the presence of root hairs and Casparian strips (Figures 3D, 3E, and S3), which were present even in severely affected roots. Hence, defects were restricted to vascular tissue, despite the expression of both *LHW* and *LL1* in other cell types (Figures 2J and 2K). Analysis of initial defects in *tmo5 t5l1 t5l2 t5l3* quadruple mutant embryos by 3D imaging (Figures 3K and 3L) showed that the phenotypes were indistinguishable from that of the *tmo5 t5l1* double mutant (Figures 1L and 1M). Consistent with the expression of *LHW* and *LL1* in globular-stage embryos (Figures 3I and 3J), *lhw ll1* double-mutant embryos showed the same primary defect in the early embryo (Figure 3M).

Importantly, although the reduced size of the vascular tissue in *tmo5 t5l1* double (Figures 3A, 3C, and S3B) or *lhw* single mutants (Figures 3A, 3F, and S3F; Ohashi-Ito and Bergmann, 2007) was stable and tissue growth was indeterminate, all higher-order mutants showed a switch to determinate vascular growth. Younger parts of higher-order mutant roots had fewer vascular cells than older parts of the same root, and the *tmo5 t5l1 t5l2 t5l3* quadruple mutant completely lost vascular tissue after ~1 week (Figure S3). To determine the cellular basis of this phenotype, we quantified the number of cells in root vascular tissue in optical cross-sections of WT *and tmo5 t5l1 t5l3* triple

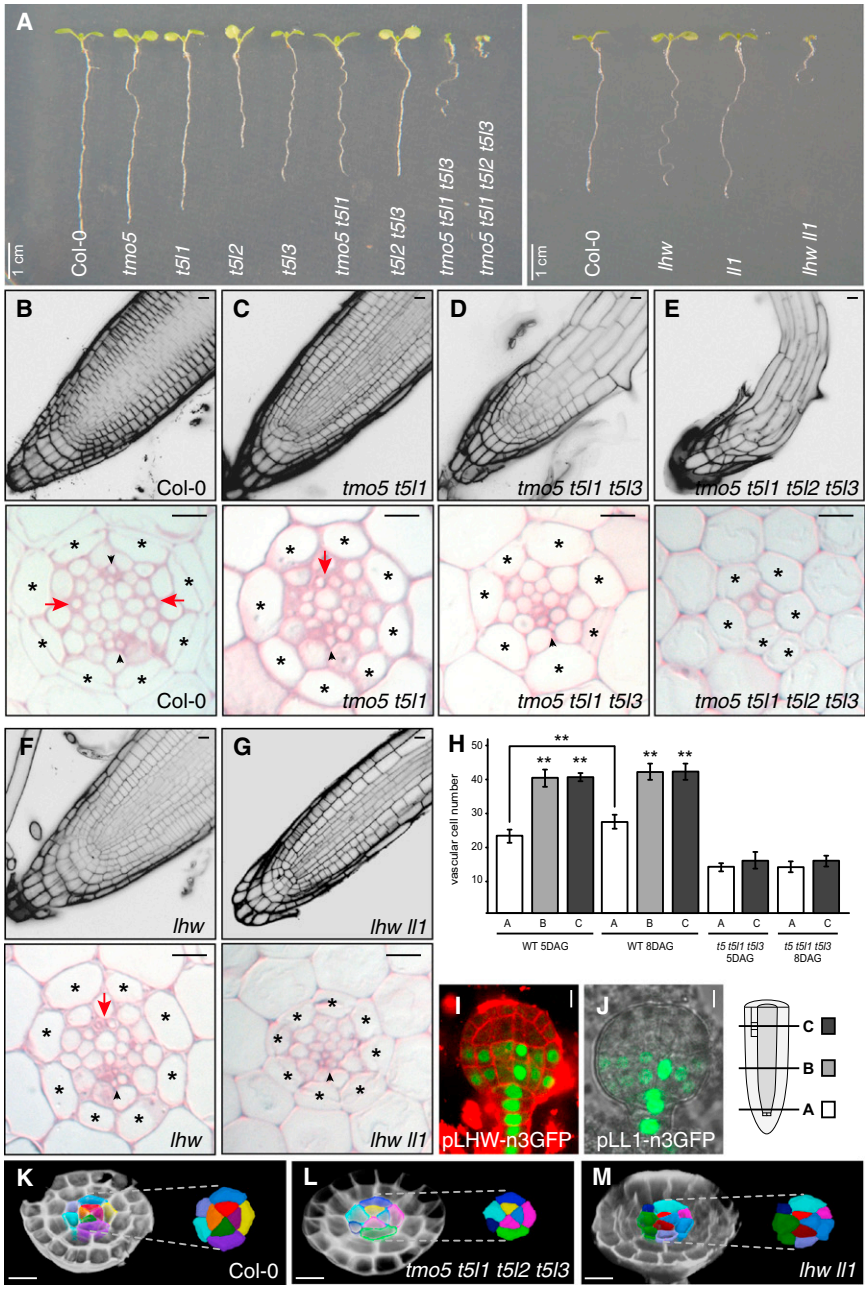

Figure 3. TMO5 and LHW Clades Are Required for Vascular Indeterminacy

(A) Seedling phenotypes of 7-day-old single and multiple mutants within *TMO5* and *LHW* clades.

(B–G) Root meristems and differentiation zone histological sections of *TMO5* and *LHW* clade single and multiple mutants. Asterisks indicate endodermis, black arrowheads indicate phloem, and red arrows mark xylem.

(H) Average number of vascular cell files in cross-sections (n = 10 roots for each genotype and stage; positions indicated in scheme) of 5- or 8-day old WT and *tmo5 t5l1 t5l3* mutant roots. Error bars in indicate SD; **p < 0.0001 for t test (A versus B or C; A-5DAG versus A-8DAG).

(I and J) Expression patterns of p*LHW-n3GFP* (I) and p*LL1-n3GFP* (J) in globular-stage embryos.

(K–M) 3D reconstructions of WT (K), *tmo5 t5l1 t5l2 t5l3* quadruple-mutant (L), and *lhw l1* double-mutant (M) embryos.

Scale bars represent 10 μm unless otherwise indicated. See also Figure S3 and Table S2.

mutants. In 5-day old WT roots (n = 10), we found 23.7 ± 2.0 vascular cell files immediately above the quiescent center (QC; Figure 3H), whereas this number was reduced to 14.6 ± 1.2 in the triple mutant. In WT meristems, the number of cell files in the vascular tissue increased to 40.4 ± 1.3 in the transition zone, which implies that ~17 periclinal divisions occurred in the meristem. By counting the number of cell files halfway through the meristem, we found that all of these periclinal divisions took place in the lower half of the meristem (Figure 3H). Strikingly, no such divisions were found in the triple mutant (Figure 3H). To determine how this defect relates to indeterminacy, we counted vascular cell file numbers at a later time point. We found that the number of cell files increased between 5 and 8 days to 27.4 ± 1.9. In contrast, no such increase was found in the triple mutant (Figure 3H). From this analysis, we conclude that periclinal divisions in the lower half of the meristem double the number of cells in the meristem and lead to a gradual increase of vascular bundle size. In addition to their role in embryonic tissue establishment, TMO5/LHW dimers are postembryonically required for these periclinal divisions, and their absence is correlated with a loss of tissue indeterminacy.

Localization of the TMO5/LHW Domain

Genetic and proteomic data demonstrate that vascular tissue establishment and subsequent indeterminacy depend on both of the interacting TMO5 and LHW proteins. To identify precisely which cells accumulate both proteins and hence are capable of forming such heterodimers, we generated a line expressing both pTMO5-TMO5-tdTomato and pLHW-LHW-YFP, and analyzed protein colocalization in embryos and roots. Consistent with the requirement of both TMO5 and LHW, we observed colocalization of both proteins in the nuclei of vascular initial cells at the midglobular stage (Figure 4A). At the heart stage, TMO5 localization became restricted to xylem precursors, whereas LHW accumulated in a broader domain with maximal levels at the distal root pole, as well as in the cotyledon primordia. Colocalization was observed in a small zone of young vascular cells in the embryonic root and cotyledons (Figures 4B and 4C). Postembryonically, pLHW-LHW-YFP protein was found in all cell types of the root meristem, but its abundance decreased gradually in cells farther away from the QC (Figure 4D). In contrast, although

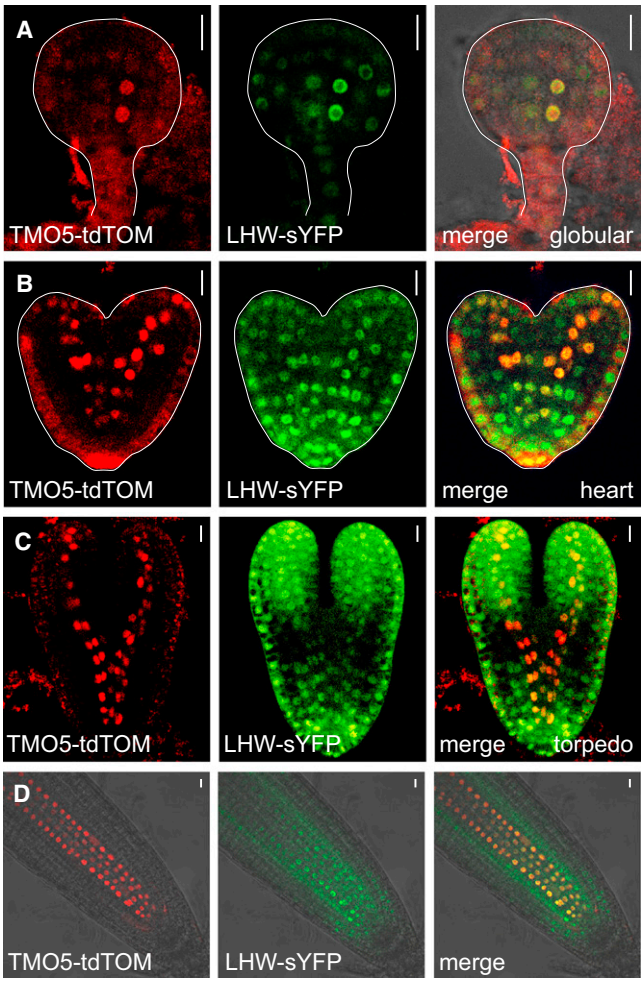

Figure 4. Overlap of TMO5 and LHW Expression Marks a Proximal Vascular Domain

Colocalization (yellow) of pTMO5-TMO5-tdTomato (in xylem precursor cells, red) and pLHW-LHW-YFP (more broadly localized, green) in globular-stage embryos (A), heart-stage embryos (B), and primary root meristems (C).

The white line marks the embryo outline; scale bar represents 10 μm. See also Figure S4 and Table S4.

pTMO5-TMO5-tdTomato protein is specific to xylem precursor cells in the root meristem, its levels remained relatively constant along the cell file (Figure 4D). Quantification of signals for both proteins and determination of relative abundance revealed a gradient of the LHW-to-TMO5 ratio along the root meristem (Figures S4A–S4C). The cells with high TMO5 and LHW levels were located close to the QC and corresponded to the zone of the root in which both TMO5 and LHW are required to mediate periclinal divisions (Figure 3H).

TMO5/LHW Triggers Periclinal Divisions

To investigate whether restriction of TMO5/LHW dimers to a small zone by transcriptional regulation is biologically meaningful, we employed a misexpression strategy. We first individually misexpressed TMO5 and LHW and their closest homologs using the strong *RPS5A* promoter (Weijers et al., 2001, 2006; Figures 5A–5C and S5A–S5I), and investigated the effect on the vascular cell population by taking in cross-sections immediately proximal to the QC. Whereas root meristems were mildly but significantly wider and shorter in pRPS5A-TMO5 plants, and no overall effect on meristem size was observed in pRPS5A-LHW roots (Figures 5A–5C, 5E, and 5H–5J), the number of vascular cell files was significantly increased in both transgenic lines (Figure 5G). Hence, transcriptional regulation of both genes restricts periclinal divisions in the vascular tissue.

If indeed TMO5 and LHW act as a heterodimer, misexpression will only be effective if the other partner is available, and individual misexpression may not reveal the full extent of TMO5/LHW function. Therefore, we simultaneously misexpressed both TMO5 and LHW using the *RPS5A* promoter. This resulted in a dramatic increase in root meristem width, with excessive cell files and layers in most tissues (Figures 5D, 5E, and 5K). Quantification of cell file number in the vascular tissue showed that the effect of joint misexpression greatly exceeded the added effects of individual misexpression (Figure 5G). This strongly supports the notion that TMO5 and LHW are mutually required within a protein complex and also suggests that no other cofactors are limiting for activity of the TMO5/LHW dimer.

The additional cell files and layers that were induced by misexpression of TMO5 or LHW, or both (Figures 5A–5D, 5J, and 5K), were accompanied by a decrease in meristem length and root growth (Figures 5E and 5H), and are consistent with the notion that the dimer is sufficient for triggering periclinal divisions. In order to exclude the possibility that the dimer increases cell divisions more generally, we counted the number of cortical cells in the meristem and found that misexpression of both TMO5 and LHW did not alter the number of anticlinal divisions compared with WT roots (Figure 5F). Additionally, the cell-cycle marker pCYCB1;1-DB-GUS (Colón-Carmona et al., 1999) showed a similar pattern in these lines when compared with WT (Figures S5H and S5I), strongly suggesting that the dimer does not promote anticlinal divisions or divisions in general. Rather, the activity is restricted to specifically promoting periclinal divisions that typically occur in the vasculature.

Although the TMO5 and LHW misexpression phenotype and loss-of-function defects are consistent with the TMO5/LHW heterodimer being necessary and sufficient for controlling periclinal cell division in tissue formation and indeterminacy, the data could also be explained by these proteins regulating an aspect of vascular identity. Therefore, we analyzed the expression of several marker genes for cell identity in the pRPS5A-TMO5/pRPS5A-LHW misexpression and *tmo5 t5l1 t5l3* triple-mutant background. We did not observe any changes in the expression of the vascular markers *Q0990* (Weijers et al., 2001), *ATHB8* (Donner et al., 2009), or *TMO5* (Schlereth et al., 2010) in single TMO5 or TMO5/LHW misexpression lines (Figures 6B, 6E, and 6H), or in *tmo5 t5l1 t5l3* roots (Figures 6C, 6F, and 6I) compared with the controls (Figures 6A, 6D, and 6G). In addition, the endodermis marker *SCR* (Heidstra et al., 2004) was normally expressed in pRPS5A-TMO5/pRPS5A-LHW as well as in *tmo5 t5l1 t5l3* roots (Figures 6J–6L), suggesting that TMO5/LHW heterodimers are not required for vascular tissue identity, and cannot impose ectopic vascular identity, but rather control periclinal cell divisions underlying indeterminacy within the vascular tissue.

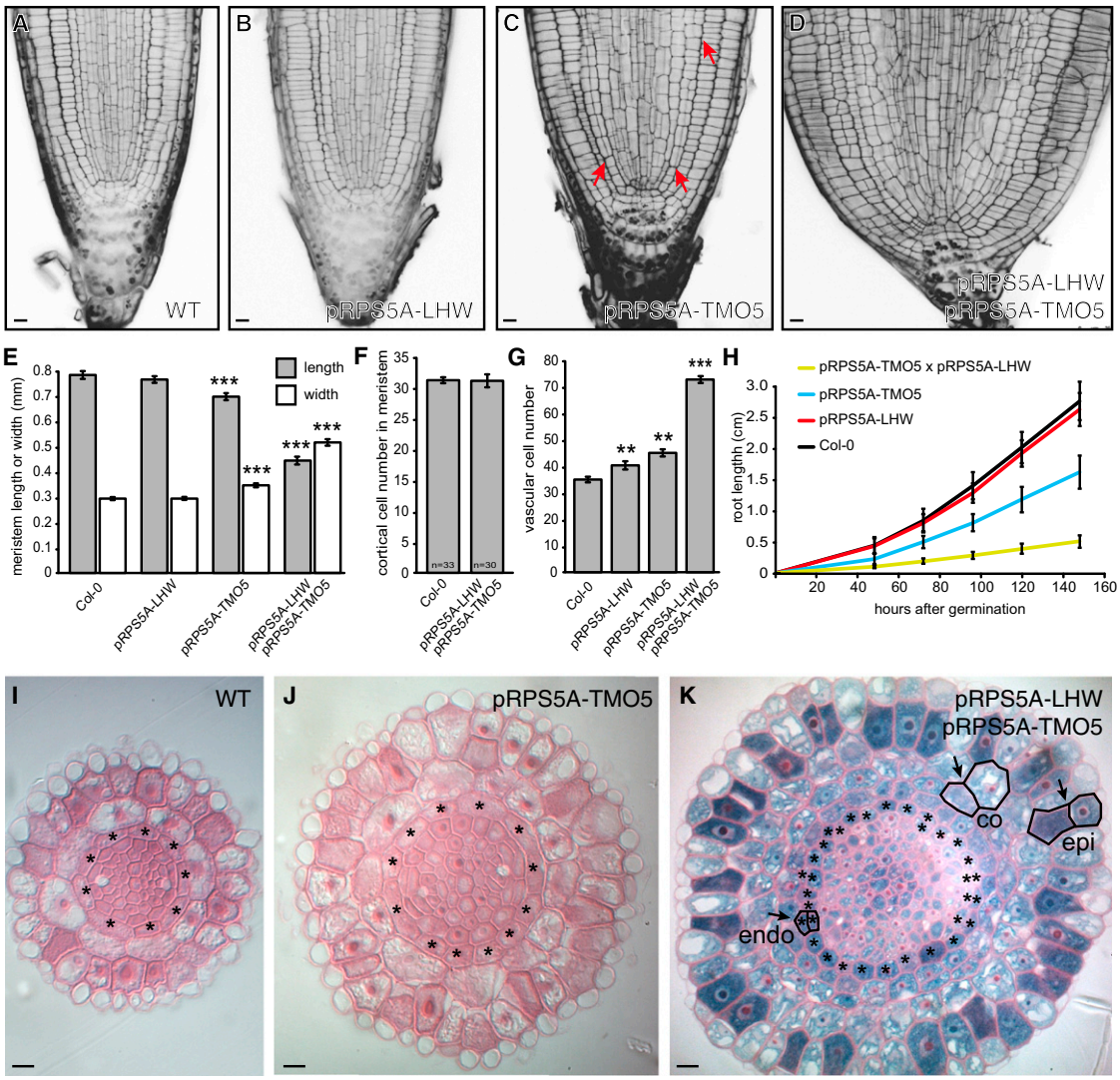

Figure 5. TMO5/LHW Dimers Trigger Periclinal Divisions

(A–H) Root meristem confocal sections (A–D), meristem length (gray), and maximal width (white, n ≥ 30) (E), cortical cell number in the meristem (n ≥ 30) (F), number of vascular cell files immediately distal to the QC in cross-sections (n ≥ 10) (G), and growth curves (n ≥ 30) (H) of WT, pRPS5A-LHW, pRPS5A-TMO5, and pRPS5A-TMO5/pRPS5A-LHW 6-day-old seedlings. Standard two-sided t test, **p < 0.001, ***p < 0.0001.

(I–K) Histological cross-sections through root meristems of WT plants (I) or plants misexpressing TMO5 (J) or both TMO5 and LHW (K). epi, epidermis; co, cortex, endo/asterisks, endodermis.

Error bars in (E)–(H) indicate SE. See also Figure S5 and Table S4.

Postembryonic Control of Vascular Indeterminacy through TMO5/LHW

Our results suggest that, after promoting vascular tissue formation in the embryo, TMO5/LHW function is required throughout development to control indeterminate growth of the root vascular tissue. An alternative interpretation, however, is that determinate vascular tissue growth results from embryonic defects that are perpetuated during postembryonic development. In this scenario, we would expect that postembryonic differences between mutants with a switch from indeterminate to determinate growth (*tmo5 t5l1 t5l3* triple and *lhw l1* double mutants) and those that are still displaying indeterminate growth (*tmo5 t5l1* double and *lhw* single mutants) are correlated with the anatomy of the vascular tissue in mature embryos. To determine whether embryonic defects explain postembryonic vascular tissue indeterminacy, we examined the number of vascular cells in mature embryos of WT and *tmo5*- and *lhw*-clade higher-order mutants (Figure 7A). Although there were fewer vascular cells in all mutants compared with the WT embryos (Figure 7A), we did not observe a difference between *tmo5 t5l1* double and *tmo5 t5l1 t5l3* triple mutants, or between *lhw* and *lhw l1* mutants. Although further reduction of TMO5 clade function, as in the *tmo5 t5l1 t5l2 t5l3* quadruple mutant, enhanced the embryonic phenotype (Figure 7A), these data show that the switch from indeterminate to determinate vascular tissue growth is not correlated with the severity of embryonic defects. Hence, we

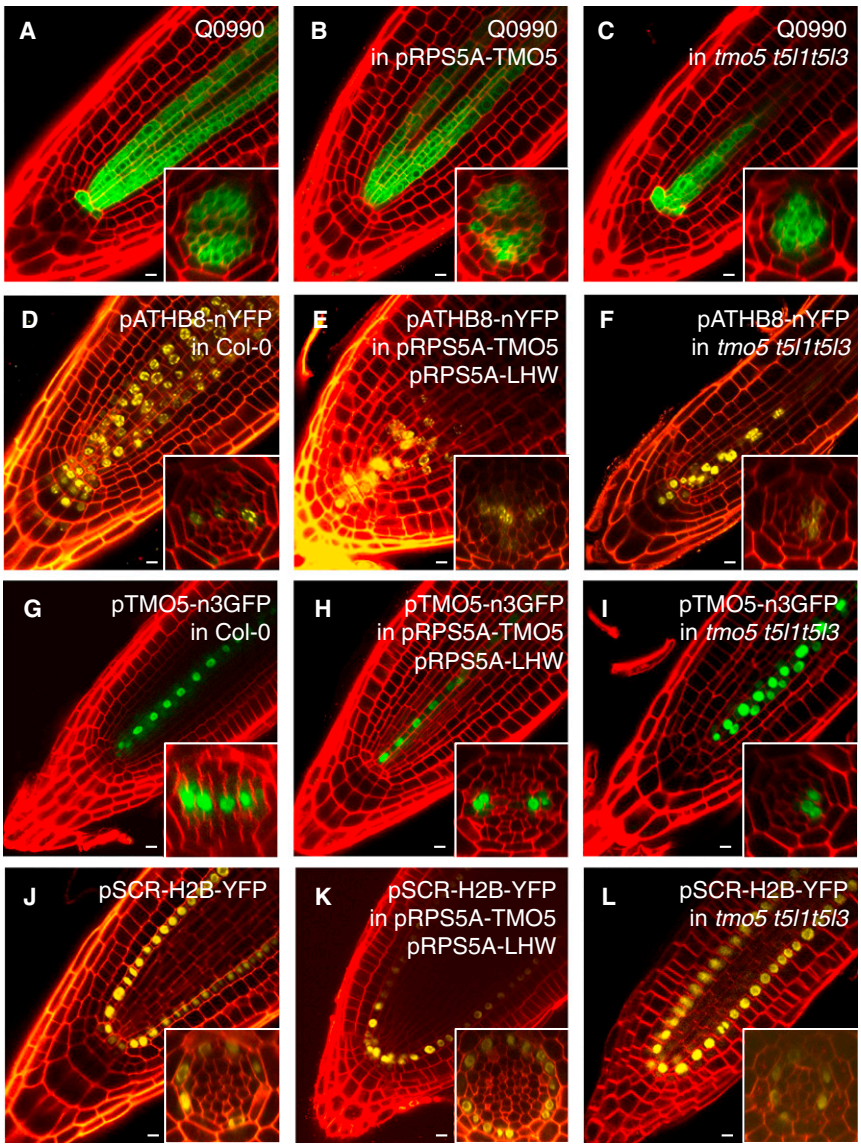

Figure 6. TMO5/LHW Does Not Regulate Vascular Cell Identities

Expression of the vascular markers Q0990 (A–C), ATHB8 (D–F), and TMO5 (G–I), and the endodermal marker pSCR-H2B-YFP (J–L) in pRPS5A-TMO5 (B), pRPS5A-TMO5/pRPS5A-LHW (E, H, and K), *tmo5 t5l1 t5l3* (C, F, I, and L), and WT (A, D, G, and J) root tips. Roots were counterstained with FM4-64 (red).

Insets show optical cross-section through the meristem. Scale bars represent 10 μm. See also Table S4.

conclude that postembryonic TMO5/LHW clade functions contribute to indeterminate vascular tissue growth.

To test more directly whether postembryonic TMO5 activity can contribute to indeterminate growth, we generated *tmo5 t5l1 t5l3* triple mutants in which pRPS5A-TMO5-glucocorticoid receptor (pRPS5A-TMO5-GR) activity could be induced by dexamethasone (DEX) treatment. When transferred to DEX-containing growth media, the narrow, determinate vascular bundle of the triple mutant (Figure 3D) was restored in these lines upon induction (Figures 7E–7G), but not in triple mutants that were not induced (Figures 7B–7D). Hence, TMO5 activity is required both embryonically and postembryonically to first generate and later maintain the vascular tissue.

The postembryonic function of TMO5 is further supported by the fact that regulation of this gene by MP is not restricted to embryogenesis, but perpetuates postembryonically. In young vascular cells in the postembryonic root, MP protein accumulates ubiquitously (Figure S6A), but MP activity (or auxin response as measured by pDR5-n3GFP expression; Weijers et al., 2006) is notably restricted to the xylem precursors (Figure S6B), in a pattern very similar to that of *TMO5* transcription (Figure 2F). Indeed, *TMO5* transcripts could be induced by brief auxin treatment in roots (Figure S6C–S6D), and *TMO5* expression is reduced in *mp* mutant seedlings and in DEX-induced bdl-GR lines (Schlereth et al., 2010; Figure S6D), demonstrating that *TMO5* is a direct postembryonic auxin-MP output in xylem precursor cells.

Non-Cell-Autonomous Control of Periclinal Divisions and Indeterminacy

Whereas TMO5 is expressed specifically in the xylem precursor cells (Figures 2F and 4D), LHW has a broader expression domain (Figures 2J and 4D). However, the similarity between the phenotypes of the *tmo5* or *lhw* clade mutants suggests that both proteins act only in the narrow domain of overlap. To test this more directly, we restored *LHW* expression in the domain marked by the *TMO5* promoter (*pTMO5-LHW*) in the *lhw* mutant. This transgene completely restored the *lhw* phenotype (Table S2), which demonstrates that both TMO5 and LHW are required only in this narrow domain.

Remarkably, although both loss- and gain-of-function data show that TMO5 and LHW are both necessary and sufficient for triggering periclinal division, the xylem cells in which the proteins accumulate do not divide periclinally (Mähönen et al., 2000). Because these divisions are observed in the surrounding procambial and phloem cells, we hypothesized that the TMO5/LHW dimer could promote periclinal divisions non-cell-autonomously in adjacent cells. Because most cell types seem to be competent for TMO5/LHW-induced periclinal division (Figures 5D and 5K), we explored whether ectopic tissue-specific induction of the dimer is capable of promoting periclinal divisions in neighboring cells. We ectopically expressed a functional, DEX-inducible TMO5-GR protein (Figures S5K–S5M) in the ground tissue using the J0571 GAL4 driver line. Because LHW was

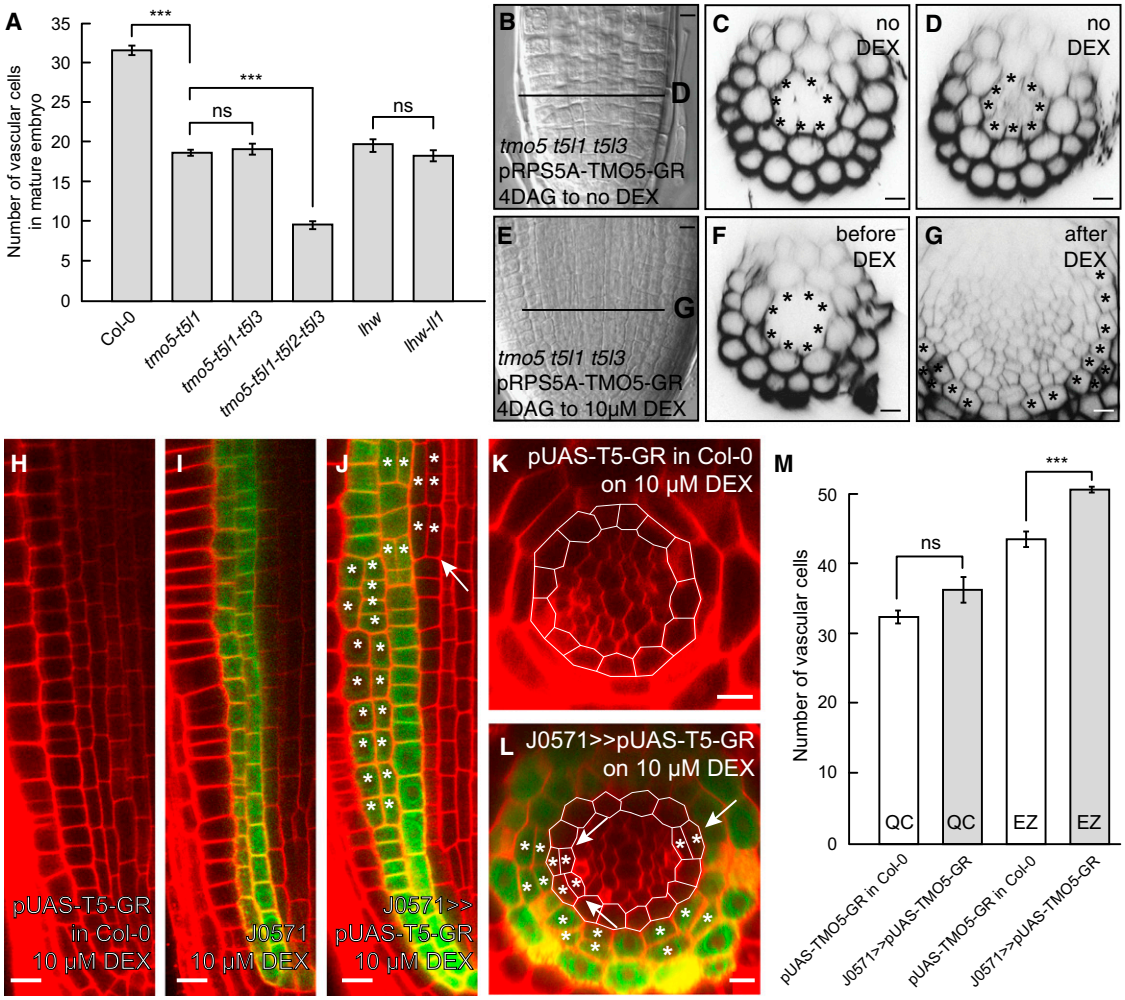

Figure 7. Postembryonic, Non-Cell-Autonomous Control of Tissue Indeterminacy

(A) Number of vascular cell files in mature embryos of WT (Col-0), *tmo5* double-, triple-, and quadruple-mutant backgrounds, and *lhw* single- and double-mutant backgrounds.

(B–G) Root tips (B and E) and cross-sections (C, D, F, and G) of the *tmo5 t5l1 t5l3* mutant carrying the pRPS5A-TMO5-GR construct, grown on control medium for 4 days and then transferred to control medium (B–D) or 10 μM DEX (E–G) for 3 more days. Cross-sections were taken before (F) and after (G) transfer.

(H–L) Confocal images of WT plants carrying the pUAS-TMO5-GR construct (H and K); J0571 control line (I) J0571 ≫ pUAS-T5-GR (J and L) grown on 10 μM DEX. Asterisks in (J) and (L) indicate additional longitudinal cell files, and arrows indicate periclinal divisions of pericycle cells. Outlines in (K) and (L) show pericycle cells.

(M) Quantification of vascular cell files of pUAS-T5-GR in WT or J0751 background grown on 10 μM DEX, just above the QC or in the elongation zone (EZ). Standard two-sided t test, ***$p < 0.01$; ns, not significant.

Scale bars represent 10 μm (B–G) and 5 μm (H–L). The error bars in (A) and (M) indicate SE. See also Figure S6 and Table S4.

already expressed in the ground tissue (Figures 2J and 4D), this strategy allowed us to ectopically induce the dimer in the ground tissue. As expected, in J0517 ≫ TMO5-GR seedlings grown on DEX, we observed excessive periclinal divisions in the ground tissue, resulting in additional cortex and endodermis cell files (Figures 7J and 7L). This was not observed either in lines carrying the same construct in WT background (Figure 7H) or in the J0571 driver line grown on DEX (Figure 7I). Importantly, we also observed a significant increase in periclinal divisions in the neighboring pericycle cells (Figure 7L) and in other vascular cells (Figure 7M). Because TMO5 protein does not appear to move (Figures S1A–S1J), these data support the existence of a TMO5/LHW-dependent non-cell-autonomous signal that moves from the xylem precursor cells to neighboring provascular cells to control periclinal divisions and indeterminate growth of the vasculature.

DISCUSSION

Our study identifies key regulators of the formation and indeterminate growth of vascular tissue in *Arabidopsis thaliana*. We have shown that the TMO5/LHW bHLH heterodimer acts immediately after tissue specification during the very first division of vascular cells in the early embryo. It controls both the establishment of a vascular tissue containing a sufficient number of cell files and the indeterminacy of this cell population in the growing

postembryonic tissue, and thus reveals a common genetic basis for these two processes. To our knowledge, this is the first demonstration of developmental continuity between embryonic tissue formation and postembryonic maintenance. Interestingly, we show that the common component of these two processes is the local control of periclinal cell division by the TMO5/LHW transcription factor dimer. Other transcriptional regulators were previously shown to control aspects of tissue formation and/or maintenance. For example, mutations in *SCARECROW* (*SCR*) and *PLETHORA* (*PLT*) genes cause determinate root growth (Galinha et al., 2007; Sabatini et al., 2003). However, in both cases the mutant defects suggest that all tissues are equally affected, which is very different from *tmo5* or *lhw* clade mutants in which only the vascular tissue loses indeterminacy. In particular, given that QC expression of *SCR* is required to maintain determinate root growth (Sabatini et al., 2003), TMO5/LHW and SCR likely act through different mechanisms to control indeterminacy. Because the cellular basis for PLT action in indeterminate root growth is not known (Galinha et al., 2007), future studies will have to resolve whether and where the functions of TMO5/LHW and PLT converge.

The overlapping expression patterns of TMO5 and LHW mark a small distal subpopulation of vascular cells with high levels of both proteins that corresponds exactly to the zone in which TMO5/LHW-dependent periclinal divisions occur. bHLH proteins are thought to require dimerization for DNA binding (Massari and Murre, 2000), and thus the relative protein levels of both partners are essential for complex formation. For example, regulation of bHLH partner accumulation is key to the formation of transcription complexes in vertebrate myogenesis (Berkes and Tapscott, 2005), B cell specification (Sigvardsson et al., 1997), and *Drosophila* sex determination (Salz and Erickson, 2010). In the latter example, the difference between one and two copies of an X-linked bHLH gene is crucial for sex determination. Hence, the combinatorial regulation of these two genes allows accurate positioning of a domain of periclinally dividing cells by both radial (*TMO5*) and longitudinal (*LHW*) restriction, and by auxin-dependent (*TMO5*) and auxin-independent (*LHW*) inputs. Therefore, our findings reveal a mechanism for specification of a plant cell population in the embryo, and in root development in general, that relies on the integration of two gene expression patterns (Figures S6E and S6F).

This work shows that the requirement for local control of the cell division plane is a critical mechanism for tissue formation and indeterminacy. The pattern and arrangement of cell types in the vascular tissue are strongly affected by both loss and gain of function of TMO5/LHW; however, our marker analysis indicates that these proteins are unlikely to have a direct role in establishing cell identity. Hence, vascular bundle size and pattern are linked by cell-division control. Smaller vascular bundles, such as in the *tmo5* or *lhw* mutants, shift to less complex patterns (monarch) or lose organization completely (higher-order mutants). On the other hand, TMO5/LHW misexpression causes larger vascular bundles with polyarch architectures. Likewise, other plant species with larger vascular bundles often have more vascular elements (Esau, 1965; McMichael et al., 1985). Additionally, it has been shown that N-1-naphthylphthalamic acid (NPA) treatment of plants can induce root vascular cell proliferation (Bishopp et al., 2011). The notion that vascular tissue patterning depends on the cell file number is supported by the finding that the vascular defect in the *wooden-leg* (*wol*) mutant (a narrow vascular cylinder with only protoxylem) can be restored by a mutation in the *FASS* gene that causes excessive division (Mähönen et al., 2000). This suggests the existence of robust self-organizing networks that pattern cell types in vascular tissues of different sizes.

Because TMO5/LHW protein coexpression is limited to the youngest xylem precursor cells in the root, it is conceivable that these cells act as a local organizer that determines the size of the vascular tissue. Indeed, the determinate vascular defect in a *tmo5 t5l1 t5l3* triple mutant can be restored by postembryonic induction of TMO5 activity, and the *lhw* mutant can be rescued by reintroducing LHW only in the TMO5 expression domain, which suggests that the TMO5/LHW dimer acts from within the xylem precursors to control tissue indeterminacy. Furthermore, when ectopically expressed in the ground tissue, TMO5 is able to induce periclinal divisions in neighboring tissues. Because TMO5 and LHW are bHLH transcription factors, and the protein does not appear to move itself, candidates for downstream mobile signals could potentially be found among the target genes. In any event, it is intriguing that TMO5 acts as a direct output of auxin activity in the xylem. It has been known for decades that auxin is sufficient for the induction of entire vascular strands (Sachs, 1981), yet auxin response is primarily observed in xylem precursors in the root meristem. Therefore, auxin-dependent cell-cell signaling through TMO5 could explain this local inductive auxin activity.

In conclusion, our work identifies key factors that control vascular tissue formation and indeterminacy. Both *TMO5* and *LHW* genes have homologs in sequenced genomes of all vascular plants, including *Selaginella moellendorffii*, but not in the (nonvascular) moss *Physcomitrella patens* (Carretero-Paulet et al., 2010; Pires and Dolan, 2010a, 2010b). The identification of the TMO5/LHW dimer as a key regulator of vascular development should now allow questions regarding the evolution of the vascular system to be addressed.

EXPERIMENTAL PROCEDURES

Plant Material

All seeds were surface sterilized, sown on solid MS plates, and vernalized for 2 days before they were grown at a constant temperature of 22°C in a growth room. T-DNA or Ds transposon insertion lines *tmo5-4* (GABI-KAT_143E03), *t5l1* (RIKEN_12-4602-1), *t5l2* (RIKEN_16-0907-1), *t5l3* (SALK_109295), *lhw* (SALK_023629), and *ll1* (SALK_108940), and Q0990 and J0571 GAL4 enhancer trap lines were obtained from the *Arabidopsis* Stock Centers (NASC-ABRC) and genotyped using the primers listed in Table S4. *mp*-B4149 and *mp*-S319 mutants were described previously (Donner et al., 2009; Schlereth et al., 2010; Weijers et al., 2005). The following reporter lines were used as described previously: pCYCB1;1-DB-GUS (Colón-Carmona et al., 1999), pSCR-H2B-YFP (Heidstra et al., 2004), pATHB8-nYFP (Donner et al., 2009), pDR5-n3GFP (Weijers et al., 2006), and pMP-MP-GFP (Schlereth et al., 2010). The AGI identifiers for the genes used in this study were as follows: TMO5/bHLH32: AT3G25710; T5L1/bHLH30: AT1G68810; T5L2/bHLH106: AT2G41130; T5L3;bHLH107: AT3G56770; LHW/bHLH156: AT2G27230; LL1/bHLH157: AT1G64625; and LL2/bHLH155: AT2G31280.

Cloning

All cloning was performed using the LIC cloning system and vectors described by De Rybel et al. (2011). For transcriptional fusions of pTMO5, pT5L1, pT5L2, pT5L3, pLHW, pLL1, and pLL2, 2–4 kb fragments upstream of the ATG were

PCR amplified from genomic DNA using Phusion Flash polymerase (Finzymes). For translational fusions, the same promoter fragment was amplified together with the genomic coding sequence excluding the stop codon. To generate pRPS5A-driven misexpression, the coding sequences of all genes were amplified from complementary DNA (cDNA) clones. To generate pRPS5A-TMO5-GR, pRPS5A-TMO5-YFP, and pRPS5A-LHW-YFP, GR or YFP was added to the cDNA by overlap extension PCR. To construct the pTMO5-LHW rescue construct, the LHW coding sequence was cloned into a pGIIB-pTMO5-LIC-NOSt vector. All constructs were completely sequenced. The primers used are listed in Table S4.

Microscopic Analysis

Differential interference contrast (DIC) microscopy, fluorescence microscopy, and confocal microscopy were performed as described previously (Llavata-Peris et al., 2011). For histological sections, roots were fixed overnight and embedded as described previously (De Smet et al., 2004). 3D imaging of embryos was performed according to Truernit et al. (2008) with the following modifications: briefly, embryos were hand-dissected from ovules before fixation and Schiff staining. Confocal image stacks were reconstructed and segmentation was performed in MorphoGraphX software (Kierzkowski et al., 2012). Confocal imaging was performed on a Zeiss LSM510 microscope or Leica SP5-II system (HyD detector). Colocalization of TMO5-tdTomato and LHW-YFP proteins was done in sequential scans using the following settings: tdTomato excitation at 561 nm and detection at 568–600 nm, YFP excitation at 514 nm, and detection at 525–550 nm.

IP-MS

IP experiments were performed as described previously (Zwiewka et al., 2011) using 3 g of siliques and/or seedlings of pTMO5-TMO5-3GFP or pLHW-LHW-YFP transgenic lines in Col-0 background for each sample. Interacting proteins were isolated by applying a total protein extracts to anti-GFP-coupled magnetic beads (Milteny Biotech). Three biological replicates of each sample were compared with three nontransgenic Col-0 samples (Table S3). MS and statistical analysis using MaxQuant and Perseus software were performed as described previously (Hubner et al., 2010; Lu et al., 2011) with minor modifications.

FRET-FLIM

FRET-FLIM analysis of *Arabidopsis* leaf mesophyll protoplasts was performed as described previously (Rademacher et al., 2011) with minor modifications. All cloning for FRET-FLIM was done using pMON999-LIC-YFP-NOSt and pMON999-LIC-CFP-NOSt vectors modified for LIC cloning (De Rybel et al., 2011) and the primers described in Table S4.

Quantitative RT-PCR Analysis

Quantitative RT-PCR analysis was performed as described previously (De Rybel et al., 2010). RNA was extracted with the RNeasy kit (QIAGEN). Poly(dT) cDNA was prepared from 1 μg of total RNA with an iScript cDNA Synthesis Kit (Biorad) and analyzed on a CFX384 Real-Time PCR detection system (BioRad) with iQ SYBR Green Supermix (BioRad) according to the manufacturer's instructions. Primer pairs were designed with the Beacon Designer 7.0 (Premier Biosoft International). All individual reactions were done in triplicate with two or three biological replicates. Data were analyzed with qBase (Hellemans et al., 2007). Expression levels were normalized to those of *EEF1α4* and *CDKA1;1*. The primer sequences are listed in Table S4.

SUPPLEMENTAL INFORMATION

Supplemental Information includes six figures and four tables and can be found with this article online at http://dx.doi.org/10.1016/j.devcel.2012.12.013.

ACKNOWLEDGMENTS

The authors thank Thomas Berleth, Enrico Scarpella, and Ykä Helariutta for sharing materials and Tom Beeckman and Sacco de Vries for their helpful comments on the manuscript. This work was supported by a long-term FEBS fellowship and a Marie Curie long-term FP7 Intra-European Fellowship (IEF-2009-252503) to B.D.R., a Swiss National Science Foundation grant (CR3213_132586) and SystemsX.ch support to R.S.S., and funding from the Netherlands Organization for Scientific Research (ALW-VIDI-864.06.012 and ALW-820.02.019) and the European Research Council (starting grant CELLPATTERN, contract no. 281573) to D.W. B.D.R and B.M. performed most of the experiments. S.Y. performed 3D imaging of TMO5 expression and vascular development. P.B.d.R. and R.S.S. developed MorphoGraphX software. B.D.R. and I.G. generated FRET-FLIM data with the help of J.W.B. S.B. performed nLC-MS/MS analyses. B.D.R, B.M., and D.W. conceived the study and wrote the paper with input from all of the authors. D.W. supervised the project.

Received: October 2, 2012
Revised: November 19, 2012
Accepted: December 20, 2012
Published: February 14, 2013

REFERENCES

Berkes, C.A., and Tapscott, S.J. (2005). MyoD and the transcriptional control of myogenesis. Semin. Cell Dev. Biol. *16*, 585–595.

Bishopp, A., Help, H., El-Showk, S., Weijers, D., Scheres, B., Friml, J., Benkova, E., Mahonen, A.P., and Helariutta, Y. (2011). A mutually inhibitory interaction between auxin and cytokinin specifies vascular pattern in roots. Curr. Biol. *21*, 917–926.

Carlsbecker, A., Lee, J.Y., Roberts, C.J., Dettmer, J., Lehesranta, S., Zhou, J., Lindgren, O., Moreno-Risueno, M.A., Vatén, A., Thitamadee, S., et al. (2010). Cell signalling by microRNA165/6 directs gene dose-dependent root cell fate. Nature *465*, 316–321.

Carretero-Paulet, L., Galstyan, A., Roig-Villanova, I., Martínez-García, J.F., Bilbao-Castro, J.R., and Robertson, D.L. (2010). Genome-wide classification and evolutionary analysis of the bHLH family of transcription factors in Arabidopsis, poplar, rice, moss, and algae. Plant Physiol. *153*, 1398–1412.

Colón-Carmona, A., You, R., Haimovitch-Gal, T., and Doerner, P. (1999). Technical advance: spatio-temporal analysis of mitotic activity with a labile cyclin-GUS fusion protein. Plant J. *20*, 503–508.

De Rybel, B., Vassileva, V., Parizot, B., Demeulenaere, M., Grunewald, W., Audenaert, D., Van Campenhout, J., Overvoorde, P., Jansen, L., Vanneste, S., et al. (2010). A novel aux/IAA28 signaling cascade activates GATA23-dependent specification of lateral root founder cell identity. Curr. Biol. *20*, 1697–1706.

De Rybel, B., van den Berg, W., Lokerse, A., Liao, C.Y., van Mourik, H., Möller, B., Peris, C.L., and Weijers, D. (2011). A versatile set of ligation-independent cloning vectors for functional studies in plants. Plant Physiol. *156*, 1292–1299.

De Smet, I., Chaerle, P., Vanneste, S., De Rycke, R., Inzé, D., and Beeckman, T. (2004). An easy and versatile embedding method for transverse sections. J. Microsc. *213*, 76–80.

Dhonukshe, P., Weits, D.A., Cruz-Ramirez, A., Deinum, E.E., Tindemans, S.H., Kakar, K., Prasad, K., Mähönen, A.P., Ambrose, C., Sasabe, M., et al. (2012). A PLETHORA-auxin transcription module controls cell division plane rotation through MAP65 and CLASP. Cell *149*, 383–396.

Donner, T.J., Sherr, I., and Scarpella, E. (2009). Regulation of preprocambial cell state acquisition by auxin signaling in Arabidopsis leaves. Development *136*, 3235–3246.

Esau, K. (1965). Plant Anatomy, Second Edition (New York: Wiley).

Galinha, C., Hofhuis, H., Luijten, M., Willemsen, V., Blilou, I., Heidstra, R., and Scheres, B. (2007). PLETHORA proteins as dose-dependent master regulators of Arabidopsis root development. Nature *449*, 1053–1057.

Hardtke, C.S., and Berleth, T. (1998). The Arabidopsis gene MONOPTEROS encodes a transcription factor mediating embryo axis formation and vascular development. EMBO J. *17*, 1405–1411.

Heidstra, R., Welch, D., and Scheres, B. (2004). Mosaic analyses using marked activation and deletion clones dissect Arabidopsis SCARECROW action in asymmetric cell division. Genes Dev. *18*, 1964–1969.

Hellemans, J., Mortier, G., De Paepe, A., Speleman, F., and Vandesompele, J. (2007). qBase relative quantification framework and software for management and automated analysis of real-time quantitative PCR data. Genome Biol. *8*, R19.

Hubner, N.C., Bird, A.W., Cox, J., Splettstoesser, B., Bandilla, P., Poser, I., Hyman, A., and Mann, M. (2010). Quantitative proteomics combined with BAC TransgeneOmics reveals in vivo protein interactions. J. Cell Biol. *189*, 739–754.

Kenrick, P., and Crane, P.R. (1997). The origin and early evolution of plants on land. Nature *389*, 33–39.

Kierzkowski, D., Nakayama, N., Routier-Kierzkowska, A.L., Weber, A., Bayer, E., Schorderet, M., Reinhardt, D., Kuhlemeier, C., and Smith, R.S. (2012). Elastic domains regulate growth and organogenesis in the plant shoot apical meristem. Science *335*, 1096–1099.

Llavata-Peris, C., Lokerse, A., Möller, B., De Rybel, B., and Weijers, D. (2011). Imaging of phenotypes, gene expression and protein localization during embryonic root formation in Arabidopsis. In Plant Organogenesis: Methods and Protocols, I. De Smet, ed. (Heidelberg, Germany: Humana Press).

Lu, J., Boeren, S., de Vries, S.C., van Valenberg, H.J., Vervoort, J., and Hettinga, K. (2011). Filter-aided sample preparation with dimethyl labeling to identify and quantify milk fat globule membrane proteins. J. Proteomics *75*, 34–43.

Mähönen, A.P., Bonke, M., Kauppinen, L., Riikonen, M., Benfey, P.N., and Helariutta, Y. (2000). A novel two-component hybrid molecule regulates vascular morphogenesis of the Arabidopsis root. Genes Dev. *14*, 2938–2943.

Massari, M.E., and Murre, C. (2000). Helix-loop-helix proteins: regulators of transcription in eucaryotic organisms. Mol. Cell. Biol. *20*, 429–440.

McMichael, B.L., Burke, J.J., Berlin, J.D., Hatfield, J.L., and Quisenberry, J.E. (1985). Root vascular bundle arrangements among cotton strains and cultivars. Environ. Exp. Bot. *25*, 23–30.

Ohashi-Ito, K., and Bergmann, D.C. (2007). Regulation of the Arabidopsis root vascular initial population by LONESOME HIGHWAY. Development *134*, 2959–2968.

Pires, N., and Dolan, L. (2010a). Early evolution of bHLH proteins in plants. Plant Signal. Behav. *5*, 911–912.

Pires, N., and Dolan, L. (2010b). Origin and diversification of basic-helix-loop-helix proteins in plants. Mol. Biol. Evol. *27*, 862–874.

Przemeck, G.K., Mattsson, J., Hardtke, C.S., Sung, Z.R., and Berleth, T. (1996). Studies on the role of the Arabidopsis gene MONOPTEROS in vascular development and plant cell axialization. Planta *200*, 229–237.

Rademacher, E., Lokerse, A., Schlereth, A., Llavata-Peris, C., Bayer, M., Kientz, M., Freire Rios, A., Borst, J., Lukowitz, W., Jürgens, G., et al. (2011). Different auxin response machineries control distinct cell fates in the early plant embryo. Dev. Cell *22*, 211–222.

Sabatini, S., Heidstra, R., Wildwater, M., and Scheres, B. (2003). SCARECROW is involved in positioning the stem cell niche in the Arabidopsis root meristem. Genes Dev. *17*, 354–358.

Sachs, T. (1981). The control of the patterned differentiation of vascular tissues. Adv. Bot. Res. *9*, 151–262.

Salz, H.K., and Erickson, J.W. (2010). Sex determination in Drosophila: the view from the top. Fly (Austin) *4*, 60–70.

Scarpella, E., and Helariutta, Y. (2010). Vascular pattern formation in plants. Curr. Top. Dev. Biol. *91*, 221–265.

Scheres, B., Wolkenfelt, H., Willemsen, V., Terlouw, M., Lawson, E., Dean, C., and Weisbeek, P. (1994). Embryonic origin of the Arabidopsis primary root and root meristem initials. Development *120*, 2475–2487.

Schlereth, A., Möller, B., Liu, W., Kientz, M., Flipse, J., Rademacher, E.H., Schmid, M., Jürgens, G., and Weijers, D. (2010). MONOPTEROS controls embryonic root initiation by regulating a mobile transcription factor. Nature *464*, 913–916.

Sigvardsson, M., O'Riordan, M., and Grosschedl, R. (1997). EBF and E47 collaborate to induce expression of the endogenous immunoglobulin surrogate light chain genes. Immunity *7*, 25–36.

Sozzani, R., Cui, H., Moreno-Risueno, M.A., Busch, W., Van Norman, J.M., Vernoux, T., Brady, S.M., Dewitte, W., Murray, J.A., and Benfey, P.N. (2010). Spatiotemporal regulation of cell-cycle genes by SHORTROOT links patterning and growth. Nature *466*, 128–132.

Truernit, E., Bauby, H., Dubreucq, B., Grandjean, O., Runions, J., Barthélémy, J., and Palauqui, J.C. (2008). High-resolution whole-mount imaging of three-dimensional tissue organization and gene expression enables the study of Phloem development and structure in Arabidopsis. Plant Cell *20*, 1494–1503.

Weigel, D., and Jürgens, G. (2002). Stem cells that make stems. Nature *415*, 751–754.

Weijers, D., Franke-van Dijk, M., Vencken, R.J., Quint, A., Hooykaas, P., and Offringa, R. (2001). An Arabidopsis Minute-like phenotype caused by a semi-dominant mutation in a RIBOSOMAL PROTEIN S5 gene. Development *128*, 4289–4299.

Weijers, D., Benkova, E., Jäger, K.E., Schlereth, A., Hamann, T., Kientz, M., Wilmoth, J.C., Reed, J.W., and Jürgens, G. (2005). Developmental specificity of auxin response by pairs of ARF and Aux/IAA transcriptional regulators. EMBO J. *24*, 1874–1885.

Weijers, D., Schlereth, A., Ehrismann, J.S., Schwank, G., Kientz, M., and Jürgens, G. (2006). Auxin triggers transient local signaling for cell specification in Arabidopsis embryogenesis. Dev. Cell *10*, 265–270.

Zwiewka, M., Feraru, E., Möller, B., Hwang, I., Feraru, M.I., Kleine-Vehn, J., Weijers, D., and Friml, J. (2011). The AP-3 adaptor complex is required for vacuolar function in Arabidopsis. Cell Res. *21*, 1711–1722.